BEST AVAILABLE COPY

DISEASE-MODIFYING ACTIVITY OF SB 242235, A SELECTIVE INHIBITOR OF p38 MITOGEN-ACTIVATED PROTEIN KINASE, IN RAT ADJUVANT-INDUCED ARTHRITIS

ALISON M. BADGER, DON E. GRISWOLD, RASESH KAPADIA, SIMON BLAKE, BARBARA A. SWIFT,
SANDY J. HOFFMAN, GEORGE B. STROUP, EDWARD WEBB, DAVID J. RIEMAN, MAXINE GOWEN,
JEFFREY C. BOEHM, JERRY L. ADAMS, and JOHN C. LEE

Objective. To evaluate the effects of SB 242235, a potent and selective inhibitor of p38 mitogen-activated protein (MAP) kinase, on joint integrity in rats with adjuvant-induced arthritis (AIA).

Methods. Male Lewis rats with AIA were orally treated either prophylactically (days 0–20) or therapeutically (days 10–20) with SB 242235. Efficacy was determined by measurements of paw inflammation, dual-energy x-ray absorptiometry for bone mineral density (BMD), magnetic resonance imaging (MRI), micro-computed tomography (CT), and histologic evaluation. Serum tumor necrosis factor α (TNFα) in normal (non-AIA) rats and serum interleukin-6 (IL-6) levels in rats with AIA were measured as markers of the antiinflammatory effects of the compound.

Results. SB 242235 inhibited lipopolysaccharide-stimulated serum levels of TNFα in normal rats, with a median effective dose of 3.99 mg/kg. When SB 242235 was administered to AIA rats prophylactically on days 0–20, it inhibited paw edema at 30 mg/kg and 10 mg/kg per day by 56% and 33%, respectively. Therapeutic administration on days 10–20 was also effective, and inhibition of paw edema was observed at 60, 30, and 10 mg/kg (73%, 51%, and 19%, respectively). Significant improvement in joint integrity was demonstrated by showing normalization of BMD and also by MRI and micro-CT analysis. Protection of bone, cartilage, and soft tissues was also shown histologically. Serum IL-6 levels were decreased in AIA rats treated with the 60 mg/kg dose of compound.

Conclusion. Symptoms of AIA in rats were significantly reduced by both prophylactic and therapeutic treatment with the p38 MAP kinase inhibitor, SB 242235. Results from measurements of paw inflammation, assessment of BMD, MRI, and micro-CT indicate that this compound exerts a protective effect on joint integrity, and thus appears to have disease-modifying properties.

SB 242235 is a new member of the pyridinyl imidazole class of compounds that has exhibited potent antiinflammatory activity (1–3). Early compounds in this class exerted this activity via inhibition of cyclooxygenase, 5-lipoxygenase, and proinflammatory cytokine biosynthesis (1). Inhibition of cytokine synthesis, however, has now been established as the primary pharmacologic action and is unrelated to the ability of the compounds to inhibit eicosanoids (4,5). Proinflammatory cytokines such as interleukin-1 (IL-1) and tumor necrosis factor α (TNFα) have been shown to play an important role in the pathogenesis of rheumatoid arthritis (RA), including inflammation (6–8), up-regulation of nitric oxide (9) and metalloproteinases (10), and bone resorption (11). The production of these cytokines from lipopolysaccharide (LPS)–stimulated human monocytes and from the human monocyte cell line THP-1 is inhibited by the pyridinyl imidazoles, with a 50% inhibition concentration (IC$_{50}$) of 50–100 nM (12,13).

Recent evidence that cytokines play a key role in acute and chronic inflammation has been provided by the demonstration that protein antagonists, such as IL-1 receptor antagonist and monoclonal antibodies to TNFα and its soluble receptor, can interfere with various acute and chronic inflammatory responses and are clinically

Alison M. Badger, PhD, Don E. Griswold, PhD, Rasesh Kapadia, PhD, Simon Blake, PhD, Barbara A. Swift, BS, Sandy J. Hoffman, BS, George B. Stroup, MS, Edward Webb, BS, David J. Rieman, BS, Maxine Gowen, PhD, Jeffrey C. Boehm, PhD, Jerry L. Adams, PhD, John C. Lee, PhD: SmithKline Beecham Pharmaceuticals, King of Prussia, Pennsylvania.

Address reprint requests to Alison M. Badger, PhD, SmithKline Beecham Pharmaceuticals. 709 Swedeland Road, King of Prussia, PA 19406.

Submitted for publication July 19, 1999; accepted in revised form September 21, 1999.

efficacious in RA (14,15). However, the need for orally active, small molecular weight compounds that would have the same effect as protein agents in inflammatory diseases is considerable.

SB 242235 and related compounds have been named cytokine-suppressive antiinflammatory drugs (CSAIDs), and the molecular target has been identified as the mitogen-activated protein (MAP) kinase homolog termed CSAID-binding protein 2 (CSBP2) (12), p38 (16), or RK (17,18). The binding of these compounds to the target CSBP/p38 protein in THP-1 cytosol and the inhibition of kinase activity for this recombinant protein has been correlated to their inhibition of cytokine biosynthesis (12,13), indicating a role for p38 in the regulation of cytokine production in response to various stimuli (19). Compounds structurally related to SB 242235 have been shown to attenuate the inflammatory components of disease in a number of animal models of acute and chronic inflammation in the absence of generalized immunosuppression (1,20,21) (examples include collagen-induced arthritis [2], adjuvant-induced arthritis [AJA] [20], and endotoxin shock [22,23]). In addition, inhibition of nitric oxide from IL-1-stimulated bovine cartilage and chondrocytes by the pyridinyl imidazole SB 203580 has recently been described (24).

SB 242235, when tested against a panel of representative protein kinases, shows a superior kinase selectivity profile in comparison with SB 203580. As reviewed by Lee et al (25), SB 203580 inhibits p38 isoform α with an IC_{50} of 48 nM (26) and p38β with an IC_{50} of 50 nM (27), as well as JNK2β1 (IC_{50} 280 nM) and c-raf (IC_{50} 360 nM) (28). However, SB 242235 is selective in that it does not inhibit ERK and JNK (up to 10 μM), which are structurally most related to p38 MAP kinase.

In this report, we have demonstrated significant antiinflammatory activity with SB 242235 in rats with AIA. This compound is a highly selective p38 inhibitor, which, unlike the earlier p38 inhibitor SB 203580 (29), has no direct effects on 5-lipoxygenase or cyclooxygenase-1 (Griswold D: unpublished observations). We have extended our previous findings in this animal model, in which we used SB 203580 (20), by examining the efficacy of SB 242235 when administered therapeutically as well as prophylactically to the AIA rat, a protocol reflecting the treatment of RA. In addition, we have utilized the advanced technology of magnetic resonance imaging (MRI) and micro-computed tomography (CT), as well as dual-energy x-ray absorptiometry (DEXA) and histology to clearly demonstrate the disease-modifying activity that a cytokine inhibitor of this compound class can have in an aggressive model of

inflammatory disease. The effects observed in this rat model of arthritis indicated that treatment with small molecular weight, cytokine-suppressive agents may well have beneficial effects in RA.

MATERIALS AND METHODS

Animals. Inbred male Lewis rats were obtained from Charles River Breeding Laboratories (Raleigh, NC). Within any given experiment, only animals of the same age were used. All experimental procedures were in accordance with protocols approved by the SmithKline Beecham Institutional Animal Care and Use Committee, and met or exceeded the standards of the American Association for the Accreditation of Laboratory Animal Care, the United States Department of Health and Human Services, and all local and federal animal welfare laws.

Materials. SB 242235 was synthesized at SmithKline Beecham (Philadelphia, PA). For in vivo experiments, SB 242235 was administered orally in 0.03N HCl–0.5% tragacanth (Sigma, St. Louis, MO). Indomethacin was from Sigma.

LPS-induced TNFα production. Normal (non-AIA) rats were orally administered SB 242235 in acidified tragacanth at various times prior to challenge with LPS (3.0 mg/kg intraperitoneally). Ninety minutes later, the animals were killed by CO_2 inhalation, and blood samples were collected by cardiac puncture into heparinized tubes and stored on ice. The blood samples were centrifuged and the plasma collected and stored at 20°C until assayed for TNFα by specific enzyme-linked immunosorbent assay (ELISA) (23).

ELISA method. TNFα levels were measured using a sandwich ELISA, which utilized a hamster monoclonal anti-murine TNFα (Genzyme, Cambridge, MA) as the capture antibody and a polyclonal rabbit anti-murine TNFα (Genzyme) as the secondary antibody. For detection, a peroxidase-conjugated goat anti-rabbit antibody (Pierce, Rockford, IL) was added, followed by a substrate for peroxidase. TNFα levels in the plasma samples from each animal were calculated from a standard curve generated with recombinant murine TNFα (Genzyme).

Induction of arthritis. AIA was induced by a single injection of 0.75 mg of *Mycobacterium butyricum* (Difco, Detroit, MI) suspended in paraffin oil, into the base of the tail of male Lewis rats ages 6–8 weeks (weights 160–180 gm). Hindpaw volumes were measured by a water displacement method on day 16 and/or day 20 (30). Test compounds were homogenized in acidified 0.5% tragacanth (Sigma) and administered orally in a volume of 10 ml/kg. Control AIA animals were administered vehicle (tragacanth) alone. Two dosing protocols were used: prophylactic dosing (3, 10, and 30 mg/kg/day) initiated on the day of adjuvant injection, and therapeutic administration (10, 30, and 60 mg/kg/day) initiated on day 10. Indomethacin was included as a positive control (0.3 mg/kg prophylactically and 0.5 mg/kg therapeutically).

Change in paw volume is presented as the mean and SEM of 10–12 animals per group, and the percentage inhibition of hindpaw edema was calculated as follows:

$$\% \text{ inhibition} = 1 - \left[\frac{AIA\ (treated)}{AIA\ (control)}\right] \times 100.$$

where AIA (treated) and AIA (control) represent the mean paw volume (in ml) (minus the value in the normal non-AIA control) in rats treated with SB 242235 and rats treated with vehicle alone, respectively. For statistical analysis, paw volumes of rats treated with SB 242235 were compared with those of the untreated AIA controls by Student's t-test.

Bone mineral density (BMD) measurement. Animals were killed on day 21 and the hindlimbs removed and fixed in 70% ethanol. BMD of the distal tibia was determined by DEXA using the Hologic QDR-1000 equipped with high-resolution scanning software (Hologic, Waltham, MA). Quality control of the instrument was carried out each day prior to sample analysis by scanning both a human anthropomorphic spine phantom (low resolution) and the lumbar portion of a rat spine (high resolution), both of which were embedded in methylmethacrylate. All high-resolution scans were carried out with the sample placed on top of an acrylic block, 1.5 inches deep. The x-ray beam was collimated to a diameter of 1.27 mm, and line spacing and point resolution were 0.25 mm and 0.127 mm, respectively. Scans were made of the distal tibia region of excised bones stored in 70% ethanol in a square plastic container. The depth of the liquid was constant for all samples and sufficient to cover the limbs by ~0.5 inches.

BMD, as well as bone mineral content (BMC) and bone area, were determined for the distal tibia. The region of interest was defined as the area between a line drawn parallel to the proximal edge of the calcaneus and a second line drawn perpendicular to the long axis of the tibia midway between the first line and the point where the tibia meets the fibula. The point of connection between the fibula and tibia had to be approximated in some samples with low BMD. The width of the region of interest was kept constant between samples.

Magnetic resonance imaging. All MRI studies were carried out on a 9.4-Tesla AMX spectrometer with micro-imaging accessories (Bruker Instruments, Billerica, MA). Coronal sections (250 μm thick) of rat tibiotarsal joints were imaged with an in-plane resolution of 70 × 70 μm. A time to recovery of 1 second and an echo time of 7.5 ms were used, with a data matrix of 256 × 256. The morphologic changes in the joint architecture of the AIA control rats were compared with those in the normal, non-AIA controls and AIA rats treated with SB 242235. The joints were graded as the percentage of joints with no protection (i.e., severe disease, similar to AIA controls), moderate protection, or significant protection (i.e., similar to normal, non-AIA control animals).

Micro-CT imaging. All x-ray micro-CT images of the intact rat ankle joints were obtained on a micro-CT scanner (Scanco Medical, Auenring, Switzerland). A total of 380 slices covering a length of 12.9 mm (34 μm thick), with an in-plane resolution of 34 × 34 μm and an integration time of 80 ms/projection. yielding a total imaging time of 5 hours, were collected from each joint. The raw micro-CT images were gauss filtered (sigma = 1.2, base = 2) and binarized using a constant threshold for all the samples. Only the region around the tibiotarsal joint was rendered for 3-dimensional display.

Histology. Tibiotarsal joints from randomly selected animals from the following 3 groups of rats were examined histologically: normal, non-AIA rats, AIA control rats, or AIA rats treated orally with SB 242235 at 60 mg/kg/day. Rats were killed on day 21 by CO_2 administration, and then the hind legs were fixed in formalin and decalcified in Cal-Rite (Richard-

Table 1. Determination of optimal pretreatment time for inhibition of LPS-induced TNFα production in rats by SB 242235[*]

Treatment	Pretreatment time, hours	TNFα, pg/ml	Inhibition. %
Vehicle	–	37,182 ± 2,791	–
SB 242235	4	11,236 ± 1,927	70[†]
	3	6,887 ± 1,997	81[†]
	2	4,318 ± 428	88[†]
	1	2,375 ± 449	94[†]

[*] A single dose of SB 242235 (15 mg/kg) or vehicle (0.5% tragacanth in 0.03N HCl) was given orally to normal rats at various times prior to challenge with lipopolysaccharide (LPS; 3 mg/kg intraperitoneally). Ninety minutes later, the animals were killed and plasma collected. Tumor necrosis factor (TNFα) levels were determined by specific enzyme-linked immunosorbent assay, and the results are expressed as the mean ± SEM of 6 rats per group.
[†] $P < 0.001$ versus treatment with vehicle alone.

Allen Scientific, Kalamazoo, MI) and the feet were removed from the legs at the distal tibial diaphysis. After routine processing, the feet were embedded and coronal sections were cut in the plane midway through the tibiotarsal and tarsotarsal joints. Sections were stained with Safranin O and counter-stained with fast green.

Bioassay for IL-6. Serum samples were collected from the rats on day 21 following CO_2 administration. IL-6 levels were determined using the previously described B9 bioassay (31). Briefly, B9 cells (5 × 10³ cells/well in 96-well, flat-bottom plates) were cultured with serial dilutions of rat serum in a final volume of 100 μl of RPMI 1640 (Flow Laboratories, Rockville, MD) containing 10% fetal bovine serum, 100 units/ml penicillin, 100 μg/ml streptomycin, and 2 mM L-glutamine (Grand Island Biological, Grand Island, NY). After 68 hours, 0.5 μCi of ³H-thymidine was added to each well and the plates incubated for 6 hours at 37°C. Cells were harvested and the radioactivity incorporated was determined. IL-6 was quantitated from a standard curve including known amounts of rat IL-6 (0.1–100 pg/ml). B9 proliferation was unaffected by any agents used in this study.

RESULTS

Inhibition of TNFα in normal rats. To determine an optimal pretreatment time for inhibition of LPS-induced TNFα production in vivo, SB 242235 at a dose of 15 mg/kg was administered orally to normal rats at various times (4, 3, 2, and 1 hours) prior to LPS challenge (3 mg/kg, intraperitoneally). TNFα production was inhibited significantly ($P < 0.001$ versus treatment with vehicle alone) at all time points (70%, 81%, 88%, and 94% inhibition, respectively) (Table 1). A median effective dose (ED$_{50}$) was determined for SB 242235 in rats at a pretreatment time of 2 hours. SB 242235 at doses of 10, 5, and 2.5 mg/kg, administered orally in normal rats, significantly inhibited the LPS-induced production of TNFα (80% [$P < 0.001$], 68% [$P < 0.001$],

178   BADGER ET AL

Table 2. Inhibition of LPS-induced TNFα production in normal rats by SB 242235*

Treatment	Oral dose, mg/kg	TNFα, pg/ml	Inhibition, %
Vehicle	–	70,661 ± 6,322	–
SB 242235	10	13,933 ± 3,027	80†
	5	22,316 ± 7,688	68†
	2.5	51,111 ± 7,318	28‡

* A single dose of compound or vehicle (0.5% tragacanth with 0.03N HCl) was given orally 2 hours prior to challenge with lipopolysaccharide (LPS: 3 mg/kg intraperitoneally). Ninety minutes later, the animals were killed and plasma collected. Tumor necrosis factor α (TNFα) levels were determined by specific enzyme-linked immunosorbent assay, and the results are expressed as the mean ± SEM of 6 rats per group. The median effective dose was calculated by linear regression analysis, to be 3.99 mg/kg, orally, with 95% confidence limits of 2.19–5.82.
† P < 0.001 versus treatment with vehicle alone.
‡ P < 0.05 versus treatment with vehicle alone.

and 28% [P < 0.05] inhibition, respectively, versus treatment with vehicle alone) (Table 2).

Effect of prophylactic and therapeutic treatment with SB 242235 in AIA rats. Paw inflammation. The effect of SB 242235 was evaluated using the prophylactic dosing protocol, in which the compound was administered to male Lewis rats starting on the day of adjuvant injection. SB 242235 was administered in acidified tragacanth on a daily basis, and paw inflammation was measured on day 20. On day 21 the animals were killed and the hindlimbs were taken for measurement of BMD and for MRI. The data in Table 3 show that SB 242235 effectively inhibited paw edema in the AIA rat, with an

Table 3. Inhibition of paw edema in rats with adjuvant-induced arthritis (AIA) by SB 242235*

Treatment group	Oral dose, mg/kg	Paw volume, ml	Inhibition, %
Normal, non-AIA	–	1.56 ± 0.03	–
Vehicle-treated AIA control	–	3.30 ± 0.18	–
SB 242235-treated AIA	30	2.33 ± 0.12	56†
	10	2.72 ± 0.19	33‡
	3	2.95 ± 0.29	20§
Indomethacin-treated AIA	0.3	2.48 ± 0.14	47†

* AIA was induced by an injection of 0.75 mg of Mycobacterium butyricum in paraffin oil (Freund's complete adjuvant) into the base of the tail of male Lewis rats. AIA rats were treated prophylactically with SB 242235 on days 0–20, and hindpaw volumes (mean ± SEM of 10 rats per group) were measured by water displacement on day 20.
† P < 0.001 versus vehicle-treated AIA controls.
‡ P < 0.01 versus vehicle-treated AIA controls.
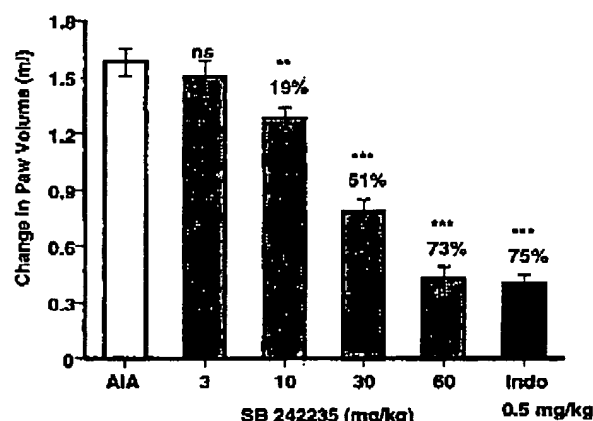§ P not significant versus vehicle-treated AIA controls.

Figure 1. Therapeutic activity of SB 242235 on paw edema in adjuvant-induced arthritis (AIA) in Lewis rats. Rats were treated with SB 242235 in acidified tragacanth at 3, 10, 30, and 60 mg/kg orally or with vehicle alone (AIA controls) from day 10 to day 20, and paw edema was measured prior to killing of rats on day 21. Values are the mean ± SEM of 12 rats per group (with inhibition expressed as a percentage of AIA controls). ** = P < 0.01 and *** = P < 0.001 versus AIA controls. ns = not significant; Indo = indomethacin.

ED_{50} of ~30 mg/kg and a minimal effective dose of 10 mg/kg.

SB 242235 was also tested in the AIA rat using a therapeutic dosing protocol, which was used to more closely represent the treatment of RA in humans. In these experiments, rats were immunized with adjuvant on day 0 and treated with compound on days 10–20 (daily). Using this protocol, hindpaw inflammation was inhibited by 73% at 60 mg/kg (P < 0.001), by 51% at 30 mg/kg (P < 0.001), and 19% at 10 mg/kg (P < 0.01) compared with treatment with vehicle alone (Figure 1). There was no activity at 3 mg/kg.

Bone mineral density. BMD was determined by DEXA using the Hologic QDR-1000 equipped with high-resolution scanning software. Scans were made of the distal tibia obtained from the animals on day 21. BMD, as well as BMC and bone area, were determined. Bone integrity of normal control rats was assigned a value of 100%, and that of AIA control rats a value of 0%. Compared with the normal, non-AIA control rats, animals treated prophylactically with 30 mg/kg and 10 mg/kg of SB 242235 showed a significant normalization of BMD and BMC. There was 49% (P < 0.001) and 23% (P < 0.05) normalization of BMD at the 30 mg/kg and 10 mg/kg doses, respectively, and a 44% (P < 0.001) and
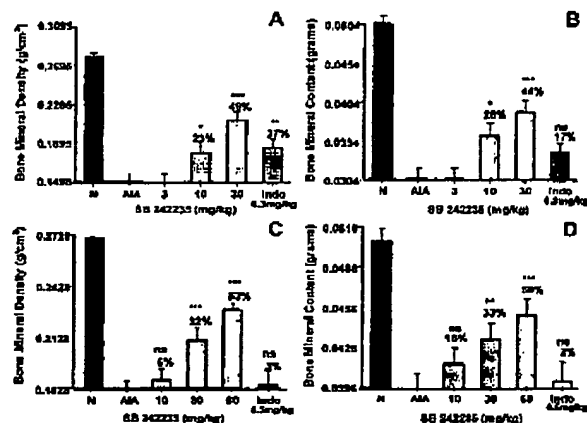
Figure 2. Bone densitometry evaluation of the distal tibia in AIA rats treated with SB 242235. Rats were treated with various doses of compound on days 0-20 (prophylactic) or days 10-20 (therapeutic). Values are the mean and SEM of 12 rats per group (with changes expressed as a percentage of normal controls [assigned a value of 100%]). A and B, Bone mineral density (BMD) and bone mineral content (BMC) of rats treated prophylactically. C and D, BMD and BMC of rats treated therapeutically. * = P < 0.05, * * = P < 0.01, and * * * = P < 0.001 versus normal controls (N). See Figure 1 for other definitions.

28% (P < 0.05) normalization of BMC, respectively, at those doses (Figures 2A and B).

Following therapeutic treatment, in which animals were dosed starting on day 10 following adjuvant injection and then dosed daily until day 20, there was also a significant normalization of BMD and BMC. There was 53% (P < 0.001) and 32% (P < 0.001) normalization of BMD at the 60 mg/kg and 30 mg/kg doses, respectively, and a 50% (P < 0.001) and 33% (P < 0.01) normalization of BMC, respectively, at these doses (Figures 2C and D).

Magnetic resonance imaging. The morphologic changes in the joint architecture of AIA rats were assessed by MRI and compared with those in normal (non-AIA) control rats and in AIA rats treated therapeutically with SB 242235. Ex vivo MR images were obtained in the intact left and right tibiotarsal joints from normal, non-AIA rats (n = 6), AIA control rats (n = 12), and AIA rats treated with SB 242235 (30 mg/kg, n = 10; 60 mg/kg, n = 12) or with indomethacin (0.5 mg/kg, n = 10). The images were ranked as showing either significant protection (no change from control), moderate protection, or no protection observed (similar to AIA controls). SB 242235 demonstrated a dose-related efficacy, with 60% of the joints being protected at 30 mg/kg and 80% being protected at 60 mg/kg
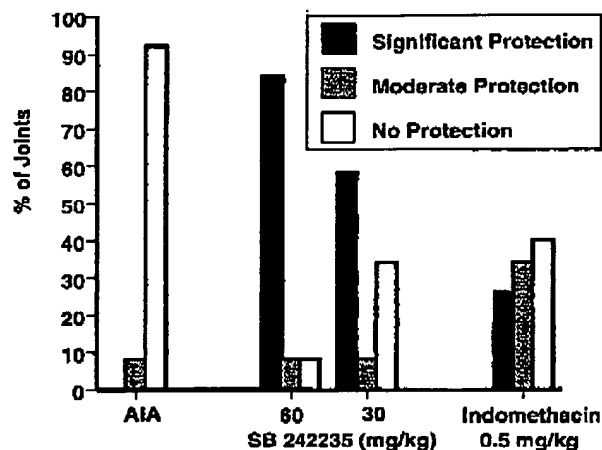

Figure 3. Magnetic resonance imaging of tibiotarsal joints of AIA rats treated therapeutically with SB 242235 (n = 10 at 30 mg/kg; n = 12 at 60 mg/kg). Data are the percentage of joints showing moderate, significant, or no protection by SB 242235 compared with AIA controls (n = 12) or normal controls (n = 6; data not shown). n = 10 AIA rats treated with indomethacin at 0.5 mg/kg. See Figure 1 for definitions.

(Figure 3). In comparison, in the indomethacin-treated group, <30% of the joints were protected.

Figure 4 shows images of joints from 4 rats from the control, non-AIA group, from the AIA control group, and from the AIA rats treated with SB 242235. The joints from the normal rats (Figure 4A) exhibited intact joint architecture. The distal tibia, fibula, and talus were well defined and there was no edema. The joints from the AIA control group (Figure 4B) exhibited
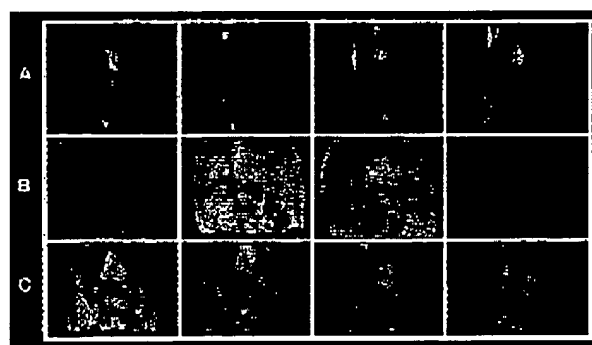

Figure 4. Representative coronal magnetic resonance images of tibiotarsal joints from A, normal, non-AIA rats; B, rats with AIA; and C, rats with AIA treated with SB 242235 at 60 mg/kg. See Figure 1 for definitions.
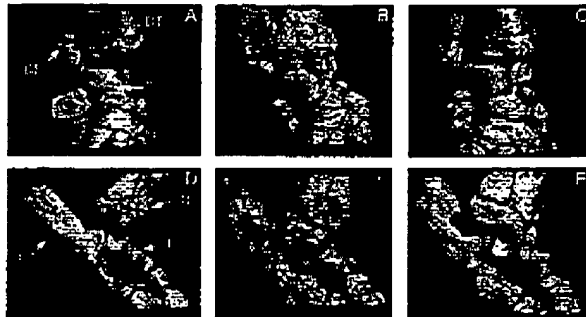
BADGER ET AL

Figure 5, Micro—computed tomography views (coronal and sagittal) of rat tibiotarsal joints rendered in representative 3-dimensional images. A–C, Coronal views of a tibiotarsal joint from a normal, non-AIA rat, an AIA control rat, and an AIA rat treated therapeutically with SB 242235 (60 mg/kg), respectively. The distal tibia (DT), distal fibula (DF). and the talus (T) can be clearly visualized in the images. Significant bone-related damage can be seen in the image of the joint from the AIA control rat as compared with the joint from the normal rat, and significant protection is apparent with SB 242235. D–F, Sagittal views of the same joints as those shown in A–C. Sagittal images afford clear visualization of the calcaneus (C), where a significant amount of destruction has taken place. Again, significant protection is afforded by treatment with SB 242235. See Figure 1 for other definitions.

significant damage as well as swelling, and there was a marked loss in cortical as well as trabecular bone. The joints from the SB 242235–treated group (Figure 4C) exhibited significant inhibition of damage, and closely resembled the joints from the normal, non-AIA controls.

Micro-CT. The micro-CT images afforded a vivid, nondestructive visualization of the bone changes that occurred over the entire tibiotarsal joint. Coronal and sagittal views of the joints are shown in Figure 5. Images of a normal rat joint (Figures 5A and D) showed intact joint architecture as well as normal bone surfaces. The various bones that constitute the joint, namely, the distal tibia/fibula, talus, and the calcaneus, were clearly resolved. The joint from the AIA control rat (Figures 5B and E) showed marked erosion of several bone surfaces, especially at the junction of the distal tibia and fibula and also along the length of the calcaneus. Degenerative changes were also visible on the talus. The images of the joint from an AIA rat treated with SB 242235 (Figures 5C and F) showed the protective effects of the compound in inhibiting the degenerative changes. Isolated regions of bone erosion could be visualized, but the integrity of the joint architecture was clearly preserved.

Histology. For histologic evaluation, randomly selected limbs from the controls and treated groups of

rats were sectioned through the tibiotarsal and tarsotarsal joints and examined for pathologic changes to the soft and connective tissues. Photomicrographs of a joint from a normal rat, a rat challenged with adjuvant and then treated with vehicle (AIA control), and from AIA
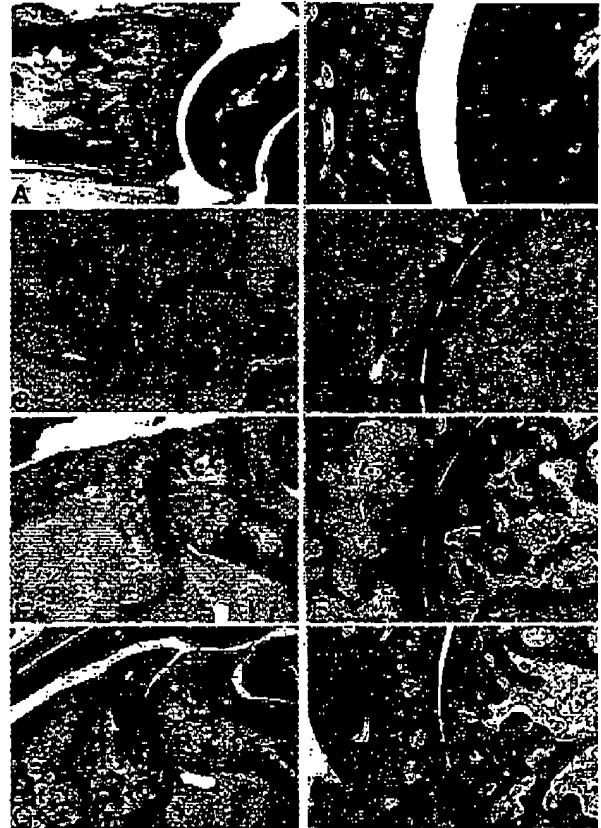

Figure 6, Photomicrographs of rat tibiotarsal joints. A and B, A normal tibiotarsal joint from a non-AIA rat. Articular cartilage is stained with Safranin O (pink), and other tissues are stained blue/green. The articulation of the distal tibia and the proximal tarsus runs vertically through the center of the image. Note the normal joint architecture. C and D, Coronal section of a tibiotarsal joint from a vehicle-treated control AIA rat. E and F, A tibiotarsal joint from an AIA rat administered 0.5 mg/kg/day indomethacin on days 10–20. Compared with the vehicle-treated AIA joint, treatment with indomethacin has limited the severity of the joint destruction. Numerous osteoclasts are evident on the subchondral bone surfaces. G and H, Coronal section of a tibiotarsal joint from an AIA rat administered 60 mg/kg/day SB 242235 therapeutically on days 10–20. Note that compared with the joint from the AIA control rat, joint integrity has been significantly maintained with SB 242235. See Figure 1 for definitions.

rats treated with either indomethacin or SB 242235 are shown in Figure 6. Joint architecture of a normal joint is shown in Figures 6A and B. In the AIA control joint (Figures 6C and D), all of the original bone and marrow had been replaced by granulation tissue and newly formed woven bone. Remnants of articular cartilage were evident and the former joint space had been infiltrated with granulation tissue. A representative joint from an AIA rat treated with indomethacin is shown in Figures 6E and F. When compared with the vehicle-treated joints, all joints examined from the indomethacin-treated group demonstrated some protection of joint integrity. Bone destruction and the replacement of marrow with granulation remained extensive throughout the tibia and tarsus. However, loss of proteoglycan from the articular cartilage was attenuated. A tibiotarsal joint from an AIA rat treated therapeutically with SB 242235 is shown in Figures 6G and H. In all of the joints examined from the rats administered SB 242235, there was a clear protective effect on the joint integrity. Treatment resulted in protection of the joint space, articular surfaces, proteoglycan loss, and subchondral bone architecture.

Serum IL-6. IL-6 has been shown to be increased markedly in different biologic fluids in patients with autoimmune disease, particularly those with RA (32–34), and the level in various inflammatory compartments appears to be a sensitive marker of disease activity. After therapeutic administration of SB 242235, there was a significant inhibition of this cytokine at the 60 mg/kg dose, but not at the lower doses (Figure 7).

DISCUSSION

The p38α MAP kinase, a member of the MAP kinase family of serine-threonine protein kinases, was first identified as a protein kinase activated in mouse macrophages in response to LPS (16). Subsequently, CSBP2, the human ortholog of p38, was identified as the molecular target of the pyridinyl imidazole class of antiinflammatory agents. The inhibition of p38 MAP kinase and subsequent inhibition of the synthesis of a number of important proinflammatory proteins has been identified as the primary mechanism contributing to the antiinflammatory activity of these compounds. Examples of inhibited cytokines are IL-1 and TNFα, IL-6, IL-8, and granulocyte-macrophage colony-stimulating factor, but not granulocyte colony-stimulating factor or IL-1 receptor antagonist (12,13,25,35).

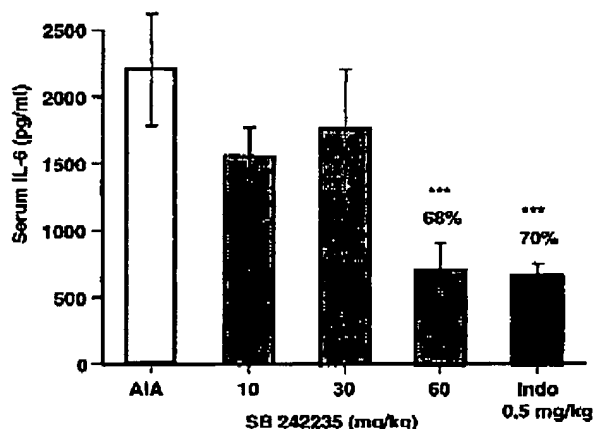The p38 pathway and the closely related JNK and

Figure 7. Inhibition of serum levels of interleukin-6 (IL-6) in AIA rats treated with SB 242235. Rats were administered SB 242235 orally from day 10 to day 20. Serum IL-6 levels were measured on day 21. Values are the mean $\pm$ SEM of 12 animals per group (with inhibition expressed as a percentage of AIA controls). *** = $P < 0.001$ versus AIA controls. See Figure 1 for other definitions.

ERK kinase signaling pathways are commonly associated with the early stages of host response to injury and infection, and their potential role in various pathologic conditions has made them targets for therapeutic intervention. The p38 MAP kinase signaling pathway is activated by a variety of stressful stimuli, including heat, ultraviolet light, LPS, inflammatory cytokines (IL-1 and TNF), and high osmolarity (16). When activated, p38 phosphorylates a number of down-stream substrates, which include kinases (MAPKAP K2 and K3, MST, MSK, PRAK) and transcription factors (CHOP, MEF2, CREB, and ATF2), and subsequently regulates the synthesis of several cytokines believed to be responsible for inflammation and tissue destruction in diseases such as RA. The pyridinyl imidazoles, by virtue of their inhibition of p38 kinase, have been shown to inhibit cytokine biosynthesis at both the transcriptional and translational level; however, at present, comprehensive mechanisms detailing all of the steps involved in cytokine regulation are unknown.

In general, the pyridinyl imidazole class inhibits the 2 splice forms of p38 (CSBP1 and CSBP2) as well as another homolog of p38 kinase, p38β2 (36), but not the closely related p38γ or p38δ, JNK, and ERK protein kinases. Although SB 203580 inhibits JNK2β1 and c-raf (28), a large number of other serine-threonine or tyrosine protein kinases are unaffected (36). Similar to SB 203580, SB 242235 inhibits CSBP/p38α MAP kinase

(IC_{50} 0.1 μM) and p38β2 MAP kinase (IC_{50} 1 μM), but not p38γ or p38δ MAP kinases. In contrast to SB 203580, SB 242235 does not inhibit JNK2β1 and ERK2 (Lee JC et al: unpublished observations). The mechanism of action of these p38 inhibitors is to compete with ATP by forming a 4-fluorophenyl binding pocket behind, and orthogonal to, the site normally occupied by the adenine ring of ATP (37).

Our previous studies with another member of this family of p38 inhibitors, SB 203580, showed it to be an effective antiinflammatory agent in the AIA rat when administered prophylactically (20), and also demonstrated that the antiinflammatory and disease-modifying activity was unlikely to be due to immunosuppression since little to no suppression was observed in mouse models of immune function (20,21). However, the evaluation of its activity when administered therapeutically, a more relevant model for RA, was not performed. In addition, although improvement in bone density by DEXA was observed, closer examination of joint integrity using imaging technologies such as MRI and micro-CT was also not performed.

In the studies described in the present report, we have shown that SB 242235 is a potent inhibitor of LPS-induced TNFα production in the plasma of normal rats. The optimal pretreatment time was 1–2 hours, although highly significant activity was seen 4 hours postdosing. SB 242235 demonstrated excellent inhibitory activity with regard to TNFα production after oral administration of a range of doses. The ED_{50} for inhibition of LPS-stimulated TNFα was 3.99 mg/kg given orally. The compound also inhibited LPS-induced TNFα production in the mouse with a potency similar to that in the rat (data not shown).

Antiinflammatory activity was observed in AIA in Lewis rats when SB 242235 was administered orally at 10, 30, and 60 mg/kg either prophylactically or therapeutically. There was a 73% inhibition of paw edema and a 53% normalization of BMD at the 60 mg/kg therapeutic dose, and 51% inhibition of paw edema with 32% normalization of BMD at the 30 mg/kg dose. This is significant activity for a small molecule cytokine inhibitor in such an aggressive arthritis model. Additional evidence for disease-modifying activity for the compound was provided by the obvious improvement observed in the MR images, in which 80% of the joints were significantly protected by treatment at the 60 mg/kg dose. In addition, micro-CT technology, which is uniquely suited for comprehensive 3-dimensional analysis of bone-related changes in the AIA rat, showed clear protection with SB 242235. This was particularly apparent in the distal tibia and the calcaneus. This is the first report describing the utility of this technology to evaluate joint integrity in the AIA rat. Histologic evaluation of representative joints showed that treatment resulted in protection of the joint space, the articular surfaces, and the subchondral bone structure, although synovial inflammation was still apparent. SB 242235 treatment at the 60 mg/kg dose also reduced circulating levels of IL-6. Previous studies in vitro have shown inhibition of IL-6 production from LPS-stimulated human monocytes, with an IC_{50} of 1.2 μM (Lee JC et al: unpublished observations).

The protection afforded by SB 242235 is considerable when compared with the nonsteroidal antiinflammatory drug (NSAID) indomethacin. Although indomethacin does have some bone-protective effects in the AIA rat, they are not significant. There was no improvement in BMD measurements compared with the arthritic controls following therapeutic treatment with indomethacin, and histologic evaluation indicated that, whereas protection of the cartilage was apparent, beneficial effects on bone were minimal. In addition, whereas NSAIDs have antiinflammatory effects in RA patients, they do not protect the bone from damage. Of particular relevance is the fact that indomethacin does not inhibit TNFα production in vitro or in vivo (Griswold D: unpublished observations), whereas this is a hallmark of CSAID activity. Inhibition of TNFα by these compounds makes them very attractive candidates for treatment of RA, particularly since inhibition of TNFα using monoclonal antibodies to the cytokine or its soluble receptor are clinically efficacious in RA (14,15).

The profile of activity described here for SB 242235 suggests strongly that orally active, small molecular weight cytokine inhibitors could provide significant benefit in the treatment of chronic inflammatory diseases such as RA.

REFERENCES

1. Lee JC, Badger AM, Griswold DE, Dunnington D, Truneh A, Votta B, et al. Bicyclic imidazoles as a novel class of cytokine biosynthesis inhibitors. Ann N Y Acad Sci 1993;696:149–70.
2. Griswold DE, Hillegass LM, Meunier PC, DiMartino MJ, Hanna N. Effect of inhibitors of eicosanoid metabolism in murine collagen-induced arthritis. Arthritis Rheum 1988;31:1406–12.
3. Marshall PJ, Griswold DW, Breton J, Webb EF, Hillegass LM, Sarau HM, et al. Pharmacology of the pyrroloimidazole, SK&F 105809. Biochem Pharmacol 1991;42:313–24.
4. Griswold DE, Hillegass LM, Breton JJ, Esser KM, Adams JL. In vivo differentiation of classical non-steroidal antiinflammatory drugs (NSAID) from cytokine suppressive antiinflammatory drugs (CSAID) and other pharmacological classes using mouse tumor

necrosis factor alpha (TNFα) production. Drugs Clin Res XIX 1993;6:243–8.

5. Boehm JC, Smietana JM, Sorenson ME, Garigipati RS, Gallagher TF, Sheldrake PL, et al. 1-substituted 4-aryl-5-pyridinylimidazoles: a new class of cytokine suppressive drugs with low 5-lipoxygenase and cyclooxygenase inhibitory potency. J Med Chem 1993;39: 3929–37.

6. Dinarello CA. Inflammatory cytokines: interleukin-1 and tumor necrosis factor as effector molecules in autoimmune diseases. Curr Opin Immunol 1991;3:941–8.

7. Arend WP, Dayer J-M. Cytokines and cytokine inhibitors or antagonists in rheumatoid arthritis. Arthritis Rheum 1990;33: 305–15.

8. Dayer JM, Demczuk S. Cytokines and other mediators in rheumatoid arthritis. Springer Semin Immunopathol 1984;7:387–413.

9. Cochran FC, Selph J, Sherman P. Insights into the role of nitric oxide in inflammatory arthritis. Med Res Rev 1966;16:547–63.

10. Werb Z, Alexander CM. Proteinases and matrix degradation. In: Kelley WN, Harris ED Jr, Ruddy S, Sledge CB, editors. Textbook of rheumatology. 4th ed. Philadelphia: WB Saunders; 1993. p. 248–68.

11. Roodman GD. Role of cytokines in the regulation of bone resorption. Calcif Tissue Int 1993;53:S94–8.

12. Lee JC, Laydon JT, McDonnell PC, Gallagher TF, Kumar S, Green D, et al. A protein kinase involved in the regulation of inflammatory cytokine biosynthesis. Nature 1994;372:739–46.

13. Gallagher TF, Fier-Thompson SM, Garigipati RS, Sorenson ME, Smietana JM, Lee D, et al. 2,4,5-triarylimidazole inhibitors of IL-1 biosynthesis. Bioorg Med Chem Lett 1995;5:1171–6.

14. Elliott MJ, Maini RN. New directions for biological therapy in rheumatoid arthritis. Int Arch Allergy Immunol 1994;104:112–5.

15. Moreland LW, Heck LW Jr, Koopman WJ. Biologic agents for treating rheumatoid arthritis: concepts and progress. Arthritis Rheum 1997;40:397–409.

16. Han J, Lee JD, Bibb SL, Ulevitch RJ. A MAP kinase targeted by endotoxin and in mammalian cells. Science 1994;265:808–11.

17. Rouse J, Cohen P, Trigon S, Morange M. Alonso-Llamazares A, Zamanillo D, et al. Identification of a novel protein kinase cascade stimulated by chemical stress and heat shock which activates MAP kinase-activated protein MAPKAP kinase-2 and induces phosphorylation of the small heat shock proteins. Cell 1994;78: 1027–37.

18. Freshney NW, Rawlinson L, Guesdon F, Jones E, Cowley S, Hsuan J, et al. Interleukin-1 activates a novel protein kinase cascade that results in the phosphorylation of Hsp27. Cell 1994; 78:1039–49.

19. Lee JC, Young PR. Role of CSBP/p38/RK stress response kinase in LPS and cytokine signaling mechanisms. J Leukoc Biol 1996; 59:152–7.

20. Badger AM, Bradbeer JN, Votta B, Lee JC, Adams JL, Griswold DE. Pharmacological profile of SB 203580, a selective inhibitor of cytokine suppressive binding protein/p38 kinase, in animal models of arthritis, bone resorption, endotoxin shock and immune function. J Pharmacol Exp Ther 1996;279:1453–61.

21. Reddy MP, Webb EF, Cassatt D, Maley D, Lee JC, Griswold DE, et al. Pyridinyl imidazoles inhibit the inflammatory phase of delayed type hypersensitivity reactions without affecting T-dependent immune responses. Int J Immunopharmacol 1994;16:795–804.

22. Badger AM, Olivera D, Talmadge JE, Hanna N. Protective effect of SK&F 86002, a novel dual inhibitor of arachidonic acid metabolism, in murine models of endotoxin shock: inhibition of tumor necrosis factor as a possible mechanism of action. Circ Shock 1989;27:51–61.

23. Olivera DL, Esser KM, Lee JC, Greig RG, Badger AM. Beneficial effects of SK&F 105809, a novel cytokine-suppressive agent, in murine models of endotoxin shock. Circ Shock 1992;37:301–6.

24. Badger AM, Cook MN, Lark MW, Newman-Tarr TM, Swift BA, Nelson AH, et al. SB 203580 inhibits p38 mitogen-activated protein kinase, nitric oxide production, and inducible nitric oxide synthase in bovine cartilage-derived chondrocytes. J Immunol 1998;161:467–73.

25. Lee JC, Kassis S, Kumar S, Badger A, Adams JL. p38 mitogen-activated protein kinase inhibitors—mechanisms and therapeutic potentials. Pharmacol Ther 1999;82:389–97.

26. Young PR, McLaughlin MM, Jumar S, Kassis S, Doyle ML, McNulty D, et al. Pyridinyl imidazole inhibitors of p38 mitogen-activated protein kinase bind in the ATP site. J Biol Chem 1997;272:12116–21.

27. Kumar S, McDonnell PC, Gum RJ, Hand AT, Lee JC, Young PR. Novel homologues of CSBP/p38 MAP kinase: activation, substrate specificity and sensitivity to inhibition by pyridinyl imidazoles. Biochem Biophys Res Commun 1997;235:533–8.

28. De Laszlo SE, Visco D, Agarwal L, Chung L, Chin J, Croft G, et al. Pyrroles and other heterocycles as inhibitors of p38 kinase. Bioorg Med Chem Lett 1998;8:2689–94.

29. Borsch-Haubold AG, Pasquet S, Watson SP. Direct inhibition of cyclooxygenase-1 and -2 by the kinase inhibitors SB 203580 and PD 98059. J Biol Chem 1998;273:28766–72.

30. Webb EF, Griswold DE. Microprocessor-assisted plethysmograph for the measurement of mouse paw volume. J Pharmacol Methods 1984;12:149–53.

31. Aarden LA, Lansdorp P, de Groot E. A growth factor for B-cell hybridomas produced by human monocytes. Lymphokines 1985; 10:175–85.

32. Houssiau FA, Devogelaer J-P, van Damme J, Nagant de Deuxchaisnes C, van Snick J. Interleukin-6 in synovial fluid and serum of patients with rheumatoid arthritis and other inflammatory arthritides. Arthritis Rheum 1988;31:784–8.

33. Swaak AJG, Rooyen A, van Nieuwenhuis E, Aarden LA. Interleukin-6 (IL-6) in synovial fluid and serum of patients with rheumatic diseases. Scand J Rheumatol 1988;17:469–74.

34. Hirano T, Matsuda T, Turner M. Excessive production of Il-6/B cell stimulatory factor-2 in rheumatoid arthritis. Eur J Immunol 1988;18:1797–802.

35. Lee JC, Votta B, Dalton BJ, Griswold DE, Bender PE, Hanna N. Inhibition of human monocyte IL-1 production by SK&F 86002. Int J Immunother 1990;VI:1–12.

36. Cuenda A, Rouse J, Doza YN, Meier R, Cohen P, Gallagher TF, et al. SB 203580 is a specific inhibitor of a MAP kinase homologue which is stimulated by cellular stresses and interleukin-1. FEBS Lett 1995;364:229–33.

37. Wang ZL, Canagarajah HJ, Boehm JC, Kassis S, Cobb MH, Young PR, et al. Structural basis of inhibitor selectivity in MAP kinases. Structure 1998;6:1117–28.